Molecular Plant Pathology

MOLECULAR PLANT PATHOLOGY (2011) 12(5), 449–461 DOI: 10.1111/J.1364-3703.2010.00683.X

Inactivation of Snt2, a BAH/PHD-containing transcription factor, impairs pathogenicity and increases autophagosome abundance in *Fusarium oxysporum*

YOULIA DENISOV[1,2], STANLEY FREEMAN[2] AND ODED YARDEN[1,*]

[1]*Department of Plant Pathology and Microbiology, The Hebrew University of Jerusalem, The Robert H. Smith Faculty of Agriculture, Food and Environment, Rehovot 76100, Israel*

[2]*Department of Plant Pathology and Weed Research, ARO, The Volcani Center, Bet Dagan 50250, Israel*

SUMMARY

The soil-borne, asexual fungus *Fusarium oxysporum* f.sp. *melonis* (FOM) is a causal agent of muskmelon wilt disease. The current study focused on the most virulent race of FOM—race 1,2. The tagged mutant D122, generated by *Agrobacterium tumefaciens*-mediated transformation, caused the delayed appearance of initial wilt disease symptoms, as well as a 75% reduction in pathogenicity. D122 was impaired in the gene product homologous to the Snt2-like transcription factor of *Schizosaccharomyces pombe*. Involvement of *snt2* in the early stage of FOM pathogenesis and its requirement for host colonization were confirmed by targeted disruption followed by quantitative reverse transcription-polymerase chain reaction analysis of *snt2* expression *in planta*. Δ*snt2* mutants of FOM and *Neurospora crassa* exhibited similar morphological abnormalities, including a reduction in conidia production and biomass accumulation, slower vegetative growth and frequent hyphal septation. In *N. crassa*, *snt-2* is required for sexual development, as Δ*snt-2* mutants were unable to produce mature perithecia. Suppressive subtraction hybridization analysis of the D122 mutant versus wild-type isolate detected four genes (*idi4, pdc, msf1, eEF1G*) that were found previously in association with the target of rapamycin (TOR) kinase pathway. Expression of the autophagy-related *idi4* and *pdc* genes was found to be up-regulated in the Δ*snt2* FOM mutant. In *N. crassa*, disruption of *snt-2* also conferred a significant over-expression of *idi4*.

INTRODUCTION

The soil-borne fungus *Fusarium oxysporum* f.sp. *melonis* Snyder & Hansen (FOM) (Nelson *et al*., 1981) causes vascular wilt disease of melon (*Cucumis melo* L.); race 1,2 is the most virulent of four known races affecting most commercial cultivars (Cohen *et al*., 1989). Targeted or random mutagenesis has been instrumental in the identification of the fungal genes involved in pathogenesis by the efficient utilization of *Agrobacterium tumefaciens*-mediated transformation (ATMT) in *F. oxysporum* (Mullins *et al*., 2001). Over the last two decades, 29 pathogenicity-related genes of *F. oxysporum* have been detected (Michielse and Rep, 2009). Interaction between plant hosts and fungal pathogens has evolved in a polyphyletic manner (Ma *et al*., 2010), involving multiple fungal and host genes, including different biosynthetic and transduction pathways. Plant colonization is a critical stage for the success of the disease cycle and several genes have been found to play an important role in this process. At least six pathogenicity-related genes of *F. oxysporum* involved in root penetration and colonization have been discovered to date: *fow1*, encoding a mitochondrial carrier protein, is required specifically for colonization (Inoue *et al*., 2002); a $Zn(II)_2Cys6$ transcription factor (TF) encoding *fow2* is required for the invasive growth of FOM (Imazaki *et al*., 2007); *frp1*, encoding an F-box protein, is involved in root penetration and colonization (Duyvesteijn *et al*., 2005); *fmk1*, a mitogen-activated protein kinase (MAPK)-encoding gene, is required for root attachment and host-invasive growth (Di Pietro *et al*., 2001); a *six1* gene encoding a small, cysteine-rich protein that is secreted by *F. oxysporum* during colonization of the xylem of its host, tomato (Rep *et al*., 2005), and a recently identified transcriptional regulator-encoding gene *sge1*, are required for parasitic growth (Michielse *et al*., 2009).

As TFs control biological processes by regulating the expression of multiple genes, their disruption may reveal novel regulatory pathways, especially in cases in which functional redundancy is present in downstream effectors. In particular, the study of TFs may also assist in the discovery of novel regulatory pathways of pathogenesis. Recently, several genes encoding TFs involved in the pathogenicity of *F. oxysporum* have been

**Correspondence*: Email: oded.yarden@huji.ac.il

Nucleotide sequence data reported here are available in the GenBank database under accession numbers HM246662 (*snt2*) and HM246663 (*rbs1*).

studied. Among them, the virulence factor ftf1 has been found to be expressed only *in planta* (Ramos *et al*., 2007), the pH-responsive TF PacC has been demonstrated to be a negative pathogenicity regulator of *F. oxysporum* (Caracuel *et al*., 2003) and XlnR has been reported to be a regulator of three xylanase genes involved in the pathogenicity of this fungus (Calero-Nieto *et al*., 2007).

Throughout their life cycle, fungi experience a vast variety of external signals which affect their development. Nutrient availability is one of the major forces of the host environment that needs to be overcome by fungi during infection. The requirement for the functional genes of FOM involved in the fundamental biosynthetic pathways of pathogenicity has been established over the last decade (Denisov *et al*., 2005; Namiki *et al*., 2001). Significant attention has also been given to the genes involved in nitrogen assimilation, with an emphasis on the involvement of GATA-type TFs in nitrogen regulation and plant pathogenesis (Bolton and Thomma, 2008). The GATA-type TF AreA is a global nitrogen regulator which, in *F. verticillioides*, has been shown to be involved in fumonisin production and the colonization of corn kernels (Kim and Woloshuk, 2008); in *F. oxysporum*, targeted disruption of the AreA homologue-encoding gene (*fnr1*) causes impaired nitrogen utilization and affects pathogenicity (Divon *et al*., 2006). One of the factors involved in the regulation of AreA is the target of rapamycin (TOR) kinase, which has been shown to activate the AreA cascade during nitrogen-limiting conditions in *Fusarium fujikuroi* (Teichert *et al*., 2006). The TOR kinase pathway is a well-conserved mechanism among eukaryotes; it mediates cell growth in response to nutrient availability (Rohde *et al*., 2001). In fungi, following nutrient-limiting conditions, the activation of heterokaryon incompatibility (*het*) genes or treatment with rapamycin, TOR kinase is repressed, allowing the activation of a range of downstream processes, one of which is autophagy (Dementhon *et al*., 2003; Pinan-Lucarre *et al*., 2003). Autophagy is a catabolic process involving the degradation of cell components by lysosomal machinery. Part of this process is characterized by the formation of double-membrane vesicles, called autophagosomes, which deliver cytoplasmic material to lysosomes. Autophagy is usually triggered by a variety of stresses and during nutrient-limiting conditions and supports cell survival (Levine and Klionsky, 2004), yet research on autophagy in filamentous fungi is in its infancy (Pollack *et al*., 2009). Autophagy has been shown to be involved in normal developmental processes, such as growth, differentiation and sexual development in *Podospora anserina* (Pinan-Lucarre *et al*., 2003), *Aspergillus oryzae* (Kikuma *et al*., 2006) and *Magnaporthe grisea* (Liu *et al*., 2007). Autophagy also plays an essential role during pathogenesis in the rice pathogen *M. grisea* (Veneault-Fourrey *et al*., 2006) and the bean pathogen *Colletotrichum lindemuthianum* (Dufresne *et al*., 1998). In *P. anserina*, over-expression of the TF-encoding gene *idi4* causes increased production of autophagosomes and leads to fungal cell death (Dementhon *et al*., 2004). *idi4* has also been identified recently among additional, less characterized, elements in the TOR/AreA-controlled fungal gene network (Schonig *et al*., 2008; Teichert *et al*., 2006). Interestingly, several genes, including the autophagy regulator *idi4*, have been found to be both nitrogen independent and TOR/AreA dependent, suggesting the existence of other regulatory elements that control *idi4* expression (Schonig *et al*., 2008).

In this study, we have characterized a novel TF-encoding gene, designated '*snt2*', and demonstrated its involvement in the pathogenicity of FOM, hyphal growth and conidiation in FOM and *Neurospora crassa*. *snt2* has been found to share the regulation of at least two genes with the TOR kinase pathway, one of which is an autophagy TF encoded by *idi4*. We have also determined that *snt2* is a positive regulator of *rbs1*, a novel gene unique to FOM, identified in this study.

RESULTS

The TF-encoding gene *snt2* is required for the pathogenicity of FOM

In order to identify novel pathogenicity-related genes in FOM, we employed a tagged mutagenesis approach on the basis of ATMT. Screening of 2000 stable transformants harbouring an insert of the pBHt2 and pKHt plasmids resulted in the recovery of five reduced-pathogenicity transformants. One of the transformants, designated 'D122', exhibited a 75% reduction in plant mortality when compared with the wild-type isolate (Fig. 1).

Using thermal asymmetric interlaced-polymerase chain reaction (TAIL-PCR), a 400-bp region flanking the integrated vector was amplified. The sequence of the FOM gene amplicon showed similarity to the *snt2* gene of *Schizosaccharomyces pombe*, and was therefore designated as '*snt2*'. The complete genomic DNA sequence of FOM *snt2* was amplified using the genome walking procedure and found to be 5.2 kb long, containing five short introns (172, 67, 104, 105 and 53 bp), encoding a protein of 1567 amino acids. The FOM *snt2* open reading frame was deduced by comparison with the sequence of *Fusarium oxysporum* f.sp. *lycopersici* (FOL) FOXG_01993.2 (http://www.broad.mit.edu) and with a 3.1-kb partial cDNA sequence of FOM *snt2*, amplified by reverse transcription-polymerase chain reaction (RT-PCR) with primers BAHfom1F/2R. The FOM Snt2 protein contains five conserved domains: a bromo-adjacent domain (BAH) located at amino acid position 205–324, three plant homeodomain Zn fingers (PHD) at positions 362–410, 752–793 and 1074–1144, and a GATA-type Zn finger at position 925–971 (Fig. 2A). CLUSTALW multiple alignment analysis of Snt2 showed that FOM Snt2 is 96%, 79% and 63% identical to proteins of FOL (FOXG_01993.2), *F. graminearum*

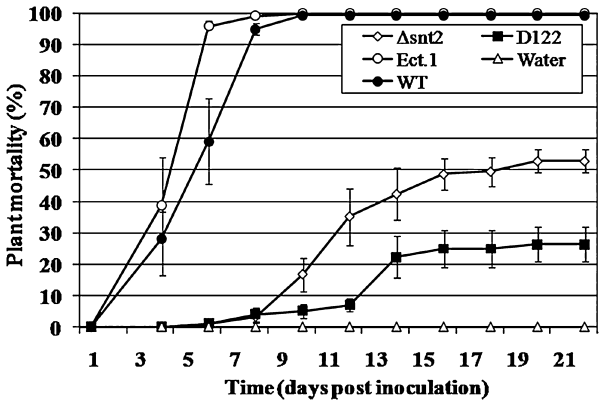

Fig. 1 Disruption of *snt2* impairs the pathogenicity of *Fusarium oxysporum* f.sp. *melonis* (FOM) on muskmelon plants. One-week-old muskmelon seedlings were inoculated by dipping the roots in a conidial suspension (5×10^5 conidia/mL) of FOM and plants were assessed for symptoms of vascular wilt disease over a 3-week period. Means and standard errors were calculated from three independent experiments and compared using the Tukey–Kramer test ($P < 0.05$). Treatments: Δ*snt2*, targeted mutant; D122, tagged mutant; Ect.1, ectopic transformant; WT, wild-type; Water, control.

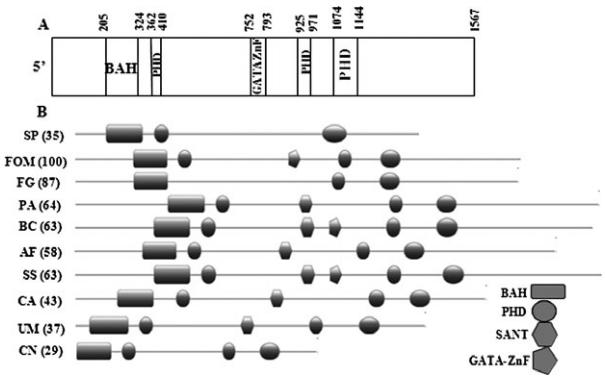

Fig. 2 SNT2 protein structure of *Fusarium oxysporum* f.sp. *melonis* (FOM). (A) The FOM Snt2 protein carries five conserved domains: a bromo-adjacent domain (BAH) at amino acid position 205–324; three plant homeodomain Zn fingers (PHD) at positions 362–410, 752–793 and 1074–1144; and a GATA-type Zn finger at position 925–971. (B) Comparison of the structural domains of SNT2 proteins between different fungi (BAH, rectangle; PHD, circle; GATA Zn finger, pentagon; SANT, hexagon). Sequences shown: SNT2 (YGL131C), *Schizosaccharomyces pombe* (SP); Snt2, *Fusarium oxysporum* f.sp. *melonis* (FOM); FOXG_01993.2, *Fusarium oxysporum* f.sp. *lycopersici* (FOL); XP_387009, *Fusarium graminearum* (FG); XP_001908700, *Podospora anserina* (PA); XP_001549253, *Botrytis cinerea* (BC); XP_750273, *Aspergillus fumigatus* (AF); XP_001584831, *Sclerotinia sclerotiorum* (SS); XP_716567, *Candida albicans* (CA); XP_761724, *Ustilago maydis* (UM); AAN75722 (ZNF1), *Cryptococcus neoformans* (CN). Similarity (percentage, in parentheses) between SNT2 of FOM and other fungi was analysed by the MatGAT program (Campanella *et al*., 2003).

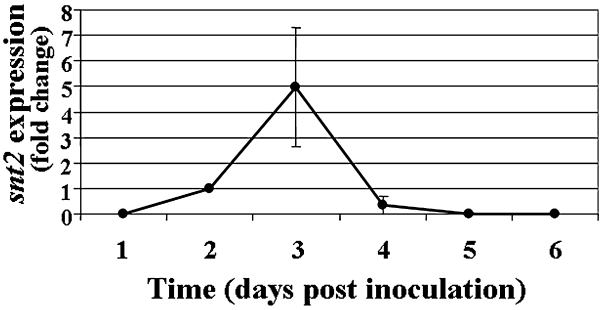

Fig. 3 Expression of *snt2* during pathogenesis of *Fusarium oxysporum* f.sp. *melonis* on muskmelon plants. cDNA was synthesized from 0.5 μg of mRNA isolated from infected plants. All samples were analysed in triplicate. Transcript levels from infected plants at 2-days post-inoculation were used as a reference. Averaged crossing point values were normalized to the endogenous control gene β-tubulin. Expression levels of *snt2* with standard error of two biological and three technical repeats were evaluated using the REST© program (Pfaffl *et al*., 2002).

(FGSG_06833.3) and *F. verticillioides* (FVEG_05152.3), respectively. The N and C termini of Snt2 displayed a lower percentage of similarity to the listed proteins. It was also found that FOXG_01993.2 contains a 60-bp 5′-untranslated region (5′-UTR); however, in FOM *snt2*, this fragment was translated, similar to that observed in FGSG_06833.3 of *F. graminearum*. Another significant difference between FOM *snt2* and its FOL homologue resides is the 84 bp shorter annotated third intron of the FOM gene compared with FOL, resulting in the translation of an additional PHD finger (Fig. 2A,B). The presence of the third PHD finger of Snt2 is common in different filamentous fungi (Fig. 2B); in *Fusarium*, it is found in the Snt2 proteins of FOM and *F. verticillioides*, but not in *F. graminearum* and FOL. The GATA-type Zn finger was only found in *F. oxysporum* and in two necrotrophic phytopathogens *Sclerotinia sclerotiorum* and *Botrytis cinerea*, but not in the other annotated fungi (Fig. 2B).

In order to determine the timing of *snt2* expression *in planta*, transcript levels of *snt2* in inoculated (infected) muskmelon plants were examined using quantitative RT-PCR over a 6-day post-inoculation (dpi) period (Fig. 3). *snt2* transcript levels became detectable at 2 dpi, most probably due to the small amount of fungal biomass within plant tissue at 1 dpi. At 3 dpi, the expression of *snt2* was five-fold higher (than at 2 dpi), whereas, at 5 dpi, *snt2* expression was significantly lower and, by 6 dpi, its expression was undetectable (Fig. 3). The first significant wilt symptoms in wild-type inoculated plants appeared at 4 dpi and, at 6 dpi, over 90% plant mortality was observed. In contrast, after inoculation with the D122 mutant, no wilt symptoms were detected until 6 dpi. Thereafter, wilt symptoms and mortality caused by D122 were evident (Fig. 1). In addition, the D122 mutant was impaired in its plant-colonizing ability and exhibited significantly lower colonization of upper plant stems

(38% ± 8%) when compared with the wild-type isolate (100%). On the basis of these results, it was concluded that the expression of *snt2* is important for invasive growth within the host and the characteristically rapid colonization of muskmelon plants.

Verification of *snt2* function by targeted gene disruption

In order to verify the significance of *snt2* in development and pathogenicity, and because, in strain D122, the mutating cassette was integrated downstream of the 5′-coding region start site, targeted gene disruption of *snt2* was performed. Approximately 200 stable transformants were obtained harbouring a 3.8-kb *snt2::hphR* wild-type gene fragment, carrying a hygromycin B resistance cassette, using ATMT (Fig. 4A). However, on the basis of the initial PCR analysis of transformant DNA, about 1% (two strains) of the isolates were confirmed to be knockout mutants. Southern blot analysis showed the presence of a single integration of the *snt2::hphR* construct at the *snt2* locus, confirming insertional mutagenesis (Fig. 4B). The transcript of *snt2* was undetectable in the Δ*snt2* isolate (as well as in the D122 strain), as determined by RT-PCR (Fig. 4C).

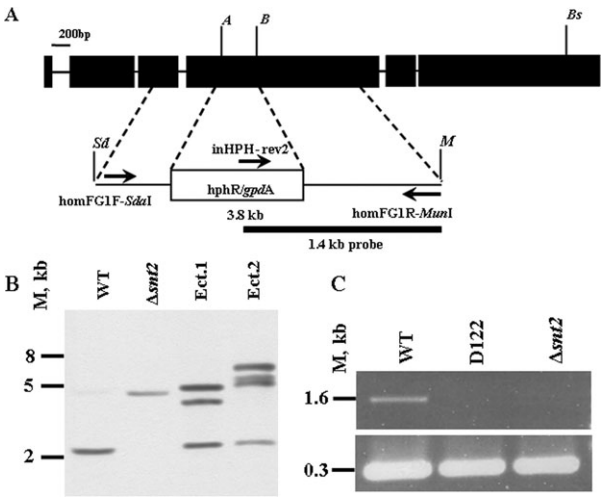

Fig. 4 Targeted disruption of *snt2* in *Fusarium oxysporum* f.sp. *melonis* (FOM). (A) The vector for targeted disruption was constructed by introducing a 2.13-kb hygromycin B resistance cassette between the *Acc65*I (*A*) and *Bgl*II (*B*) sites of a 1.6-kb fragment of FOM *snt2*, amplified with homFG1F/R primers and cloned into pGEM-T Easy, creating a 3.8-kb *snt2::hphR* cassette. The *SdaI* (Sd)/*MunI* (M) *snt2::hphR* cassette was transferred into the *EcoRI*/*PstI* binary vector pDHt in order to perform *Agrobacterium*-mediated transformation. (B) Southern blot analysis using a 1.4-kb fragment of *snt2::hphR* amplified with inHPH-rev2/homFG1R, used as a probe (see A), was performed on *Acc65*I/*Bsp1407*I (*Bs*)-digested genomic DNA, detecting a disruption of *snt2* in one transformant (designated Δ*snt2*). Ectopic transformants (Ect.1 and Ect.2) with several insert copies and a wild-type (WT) with an original *snt2* copy are also shown. (C) Reverse transcription-polymerase chain reaction (RT-PCR) analysis of *snt2* transcripts with the β-tubulin gene used as a control. M denotes DNA size in kilobases.

Plant pathogenicity assays with the Δ*snt2* mutant showed that the mutants exhibited impaired pathogenicity, as evident from the significant delay in initial symptom appearance, compared with the wild-type and ectopic transformant (Fig. 1). Furthermore, inoculation of muskmelon plants by Δ*snt2* caused a reduction by approximately 50% in plant mortality compared with the wild-type isolate, which was also significantly higher than that of the mutant isolate D122. With regard to colonization ability, Δ*snt2* demonstrated significantly decreased upper and lower stem colonization when compared with the wild-type (27% ± 8% and 59% ± 11%, respectively). Similar results were observed with the second *snt2* gene disruption strain, designated '3(15)' (data not shown). Overall, these results confirm the requirement of *snt2* for invasive pathogenic growth, and thus for full pathogenicity of FOM.

snt2 is required for fungal growth and development

In addition to the reduction in pathogenicity, cultures of both D122 and Δ*snt2* mutants of FOM also exhibited defects in growth and development. The affected parameters examined included the linear growth rates, conidia production on solid medium and biomass accumulation in minimal liquid medium (Table 1). The phenotypic analysis of the second *snt2* knockout mutant [isolate 3(15)] detected no significant differences in the parameters described above (Table 1).

In order to evaluate whether the involvement of *snt2* in development is restricted to FOM, or can be observed in another fungal species, a partial characterization of the phenotypic consequences of *snt2* disruption was assessed in the model fungus *N. crassa*. During growth on solid medium, the Δ*snt-2* strain (NCU07412.4) produced a thick, significantly slow-growing (1.65 ± 0.38 mm/h) mat of hyphae with little aerial hyphae, when compared with the normal growth attributes (2.23 ± 0.14 mm/h) of the wild-type isolate (Fig. S1, see Supporting Information). Macroconidia production of the Δ*snt-2* strain was only 10% of that of the wild-type strain [$(0.28 \pm 0.04) \times 10^9$ and $(2.19 \pm 0.37) \times 10^9$ conidia/flask, respectively], which explains the less pronounced orange colour of its mycelium (Fig. S1). In this model organism, disruption of *snt-2* also affected perithecia formation, as the Δ*snt-2* mutant strains were unable to produce mature perithecia, indicating the requirement of *snt-2* for sexual development in *N. crassa*.

Disruption of *snt2* causes increased hyphal septation in FOM and *N. crassa*

In light of the fact that *snt2* mutants exhibited slower linear growth, cell wall morphology was examined microscopically. The

Table 1 Effect of *snt2* disruption on developmental parameters of *Fusarium oxysporum* f.sp. *melonis* (FOM). Different letters (in parentheses) define significantly different groups.

Isolate	Radial growth rate (mm/day)*	Conidia production ($\times 10^4$ conidia/cm^2 colony)	Biomass accumulation (mg/25 mL)
Wild-type	7.2 ± 1.0 (a)	12.7 ± 1.7 (a)	94.6 ± 8.2 (a)
D122	4.3 ± 1.2 (b)	6.2 ± 1.2 (b)	65.7 ± 5.2 (b)
Δ*snt2*	3.5 ± 1.1 (b)	2.0 ± 0.7 (b)	62.8 ± 7.7 (b)
3(15)	3.4 ± 0.2 (b)	0.6 ± 0.1 (b)	58.7 ± 4.8 (b)

*Comparative analyses of the linear growth rate and conidial production of FOM *snt2* mutants [D122 and the Δ*snt2* mutant, as well as an additional confirmed *snt2* disruptant, 3(15)] and the wild-type isolate were performed on cultures grown on potato dextrose agar (PDA) medium. Biomass accumulation was examined after incubation in *Fusarium* minimal liquid medium (FMM). Standard errors and statistical differences [($P \leq 0.05$) in parentheses] were calculated on the basis of three independent experiments by the Least Significant Difference (LSD) Tukey-Kramer multiple comparison test.

cell wall-binding stain Congo red was employed for this purpose, enabling the detection of irregularities in hyphal septation. Distances between septa along the hyphal cells of the Δ*snt2* FOM and Δ*snt-2 N. crassa* mutants were markedly shorter than in the respective wild-type strains (Fig. 5).

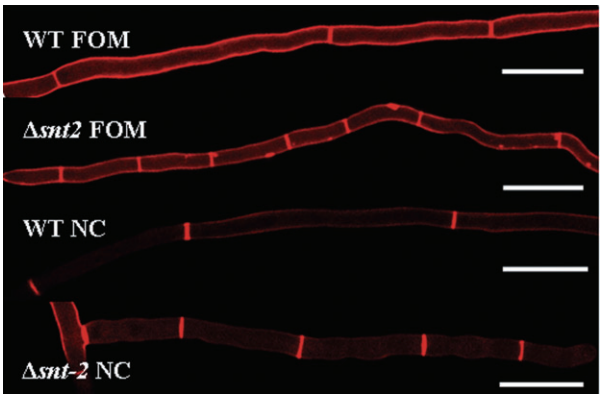

Fig. 5 *snt2* disruption leads to abnormalities of hyphal septation in *Fusarium oxysporum* f. sp. *melonis* (FOM) and *Neurospora crassa* (NC). Congo red staining detected irregularities in cell wall deposition and shorter hyphal segments between septa in the Δ*snt2* mutant of FOM and the Δ*snt2* mutant of NC, compared with their respective wild-type strains. Bars indicate 50 μm.

In vivo viability staining detected increased cell death in Δ*snt2* mutants of FOM and *N. crassa*

The first evidence of increased cell mortality caused by *snt2* disruption was detected using Evans blue staining of FOM isolates (Fig. 6A–C), suggesting that disruption of *snt2* leads to decreased cell viability. Furthermore, the ratios between stained and unstained cells in Δ*snt2* of FOM and *N. crassa* were determined. Increased cell mortality was evident in the Δ*snt2* mutants of both tested fungi, when compared with the wild-type isolates (Fig. 7), thus confirming the requirement of *snt2* for normal cell activities.

Additional morphological abnormalities detected in *F. oxysporum*

To further explore the potential mechanism involved, cells were stained with the autophagosome-detecting stain monodansylcadaverine (MDC), with and without the addition of the serine protease inhibitor phenylmethanesulphonylfluoride (PMSF), which has been shown to decrease the fast degradation of autophagosomes (Pollack *et al*., 2009). In the absence of PMSF, it was evident that mutant isolates D122 (Fig. 6E) and Δ*snt2* (Fig. 6F) contained increased amounts of MDC-stained organelles, presumably mature autophagosomes, when compared with the wild-type isolate (Fig. 6D). The addition of PMSF enhanced the appearance of MDC-stained organelles in all observed isolates (Fig. 6G–I). In order to verify the nature of these organelles, 3-methyladenine (3-MA), a specific inhibitor of autophagosome assembly (Pollack *et al*., 2009), was applied prior to MDC staining. As the presence of 3-MA almost eliminated MDC staining (Fig. 6J), it is plausible to assume that the organelles observed were autophagosomes (Fig. 6K).

Identification of differential gene expression when FOM *snt2* is impaired

Suppressive subtraction hybridization (SSH) was used to detect differentially expressed genes between the wild-type and D122 isolates of FOM. Sequences of 200 random clones were analysed, identifying 14 putative genes. Over 15% of the transcript sequences analysed did not have matches in existing databases. Association between four of the SSH-detected genes (*idi4*, induced during incompatibility; *pdc*, pyruvate decarboxylase; *msf1*, transporter of the major facilitator family; *eEF1G*, eukaryotic translation elongation factor 1-γ) and the highly conserved TOR serine/threonine kinase pathway in the rice pathogen *F. fujikuroi* has been reported previously (Teichert *et al*., 2006). The TOR pathway controls numerous cellular processes, including the regulation of cell growth through nutrient sensing. Quantitative RT-PCR was used to further investigate the expression of these genes. Two of the mentioned genes (*idi4* and *pdc*) exhibited a significant change in transcript levels in the Δ*snt2* mutant when compared with the wild-type isolate (Table 2).

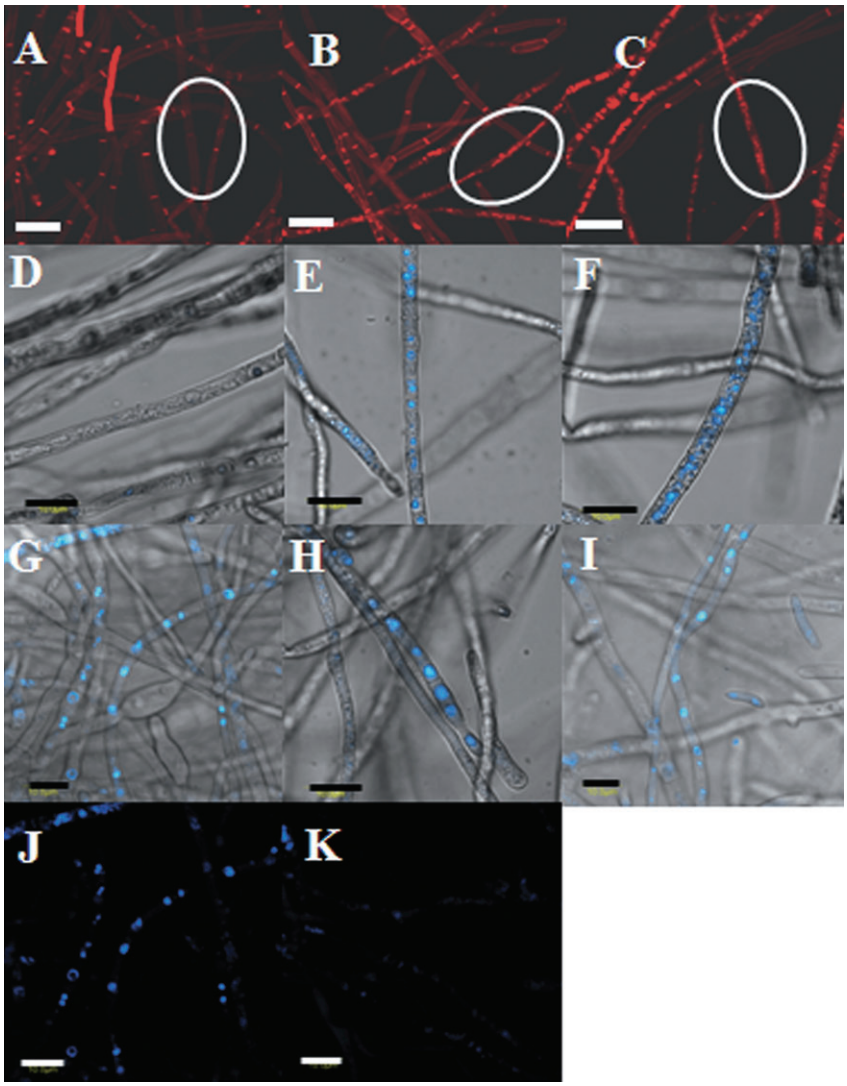

Fig. 6 Morphological abnormalities observed in *snt2* mutants of *Fusarium oxysporum* f.sp. *melonis* (FOM). Comparative analysis between Evans blue-stained mycelial cells of the wild-type isolate (A) and *snt2* mutant strains detected decreased viability of the cells in mutants D122 (B) and Δ*snt2* (C) of FOM (areas marked by circles). Monodansylcadaverine (MDC) staining of autophagosomes detected significant differences between the wild-type (D) and the mutant isolates D122 (E) and Δ*snt2* (F). Formation of autophagosomes in the presence of phenylmethanesulphonylfluoride (PMSF) and stained by MDC in the wild-type isolate (G), D122 (H) and Δ*snt2* (I) mutant isolates. Elimination of MDC staining in PMSF-treated wild-type cells (J) after addition of the specific autophagosome inhibitor 3-methyladenine (K). Bars in A–C indicate 50 μm, whereas those in D–K indicate 10 μm.

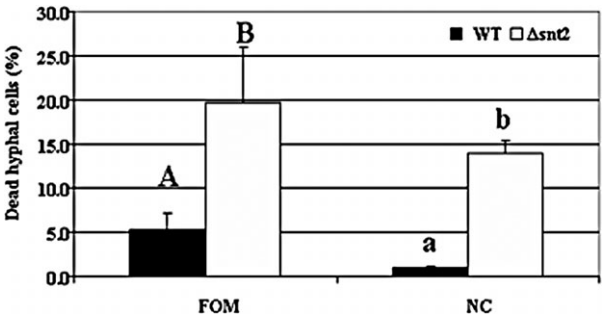

Fig. 7 *snt2* disruption leads to increased cell death in *Fusarium oxysporum* f.sp. *melonis* (FOM) and *Neurospora crassa* (NC). Percentage of dead cells in the Δ*snt2* mutants of FOM and NC, compared with their respective wild-type (WT) isolates. Results represent the mean of three independent experiments (each with 1000 cells observed), analysed separately for each fungal species by Least Significant Difference (LSD) Tukey-Kramer multiple comparison test ($P \leq 0.05$); the levels of significance are marked with different letters.

The *pdc* gene encodes a key enzyme in pyruvate assimilation, and its expression was found to be negatively regulated by TOR kinase in *F. fujikuroi*. In this study, a 20.78 ± 7.04-fold increase in *pdc* expression in Δ*snt*2 was identified, compared with the wild-type isolate; however, in the D122 mutant, *pdc* expression did not differ significantly from that of the wild-type (0.90 ± 0.13), even though this gene was detected in the suppression library of mutant isolate D122. We presume that this difference may be linked to the nature of the *hph*R cassette integrated site in the tagged D122 mutant. Another examined gene encoding a transporter of the major facilitator superfamily (*mfs*) is known to be negatively regulated by AreA (Schonig *et al*., 2008). However, its relative expression in the D122 and Δ*snt2* mutant isolates was no different from that of the wild-type isolate (1.32 ± 0.62- and 1.60 ± 0.86-fold, respectively). Furthermore, expression of an additional SSH-detected gene, *eEF1G*, encoding a translation elongation factor, which is negatively regulated by TOR kinase,

Table 2 Expression profile of nitrogen metabolism-related genes in the Δ*snt*2 mutant of *Fusarium oxysporum* f.sp. *melonis* (FOM).

Gene	Accession number	Wild-type/Δ*snt*2 expression ratio*	Description
idi4†	FOXG_04081	24.5 ± 2.25^{+}	Induced during incompatibility
cpc1	FOXG_05954	2.12 ± 0.09	Cross-pathway control
pdc†	BAE98181.1	20.78 ± 7.04^{+}	Pyruvate decarboxylase
fnr1	DQ387858	1.2 ± 0.15	Global nitrogen regulator
nit4	FOXG_06396	0.95 ± 0.08	Pathway-specific nitrogen regulator
glnA	FOXG_05182	4.02 ± 0.50	Glutamine synthetase
mfs1†	FOXG_09760	1.60 ± 0.86	Transporter of the major facilitator family
rbs1†	FOXG_14252	0.15 ± 0.03^{-}	Unknown functions
eEF1G†	FOXG_01492	2.72 ± 1.21	Translation elongation factor

*cDNA was synthesized from 1 μg of total RNA. All samples were analysed in triplicate. Averaged crossing point values were normalized to the endogenous control gene β-tubulin. Gene expression level and comparative analyses (*) of two biological and four technical repeats were evaluated using the REST© program (Pfaffl *et al*., 2002). Accession numbers were according to http://www.broad.mit.edu and National Center for Biotechnology Information (NCBI) databases. Statistically significant changes are marked by + = up-regulated and − = down-regulated.

†Identified by suppressive subtraction hybridization (SSH) screen.

was not significantly different in mutant isolate Δ*snt2* (2.72 ± 1.21-fold) when compared with the wild-type isolate (Table 2).

In addition, a unique *F. oxysporum* gene (designated *rbs1*—regulated by s*nt2*) was found. This gene encodes a 170-amino-acid protein with an as yet unknown function, and the only currently known homologue of this gene is a unique gene of FOL (FOXG_14252.2). *rbs1* expression was significantly decreased in isolates D122 and Δ*snt2* (–6.78 ± 0.37- and –8.47 ± 0.15-fold, respectively) when compared with the wild-type isolate.

Snt2 TF is involved in the regulation of the autophagy-induced TF Idi4

On the basis of SSH analysis, disruption of *snt2* led to over-expression of the putative FOM *idi4* gene. FOM Idi4 is similar (69%) to its *P. anserina* homologue IDI4, which has been shown to be involved in the regulation of autophagy (Dementhon *et al*., 2004). Using quantitative RT-PCR analysis, significantly elevated *idi4* expression was detected in D122 and Δ*snt2* FOM mutants (20.53 ± 2.04- and 24.5 ± 2.25-fold, respectively). This was also observed in *N. crassa*, where an increase in *idi4* expression (8.36 ± 0.65) was detected in the Δ*snt2* strain, suggesting a common regulatory pathway in the two fungal species.

Moreover, a significant increase in the presence of mature autophagosomes was detected in mutant D122 and Δ*snt2* isolates by MDC staining, as well as increased amounts of nonvital cells in both D122 and Δ*snt2*, compared with the wild-type isolate of FOM (Fig. 6D–K). To detect whether *snt2* is involved in direct regulation of the autophagy process, the expression of a highly conserved gene, *idi7/agt8*, which regulates the initial steps of nonselective autophagy, was examined (Levine and Klionsky, 2004). Its relative expression in the Δ*snt2* and D122 isolates (1.07 ± 0.55- and 0.59 ± 0.35-fold, respectively) was not significantly different from that of the wild-type; therefore, it is likely that *snt2* is not directly involved in the regulation of nonselective autophagy.

To investigate a possible involvement of *snt2* in nitrogen metabolism and to detect its possible connection with the TOR kinase pathway, the effect of the specific TOR inhibitor rapamycin on the utilization of different sole sources of nitrogen (nitrate, ammonia and glutamate) was examined. During growth on these three nitrogen sources, both *snt2* mutants grew in an apparently indistinguishable manner compared with the wild-type isolate. However, closer examination of radial growth showed that, initially, glutamate slightly delayed the vegetative growth of both *snt2* mutants in the absence of rapamycin and, secondly, the addition of rapamycin did not delay nitrogen utilization of the Δ*snt2* isolate, as opposed to the apparently normal growth of the tagged transformant D122 (data not shown). As demonstrated previously, both *snt2* and *areA* appear to regulate the expression of at least two common genes (*idi4* and *pdc*); therefore, we examined the transcript levels of three master nitrogen regulators [*fnr1* (a homologue of *are*A in *F. oxysporum*), *nit*4 (the homologue of a pathway-specific nitrogen regulator of *N. crassa*) and *glnA* (glutamine synthetase)] as well as the *cpc1* (cross-pathway control 1) gene, which regulates fungal amino acid biosynthesis and is negatively regulated by AreA (Schonig *et al*., 2008). Unexpectedly, the expression of these genes did not differ significantly in the Δ*snt2* mutant when compared with the wild-type isolate (Table 2). The growth of both mutant isolates was also not affected by 3-aminotriazole (3-AT), which induces the amino acid starvation response (data not shown) together with the expression of *cpc1*, supporting the results obtained by quantitative RT-PCR. Moreover, all the examined isolates were unable to utilize chlorate (6%) and did not grow on hypoxanthine (0.05%), indicating the absence of defects in the nitrate

reduction pathway. On the basis of these results, it is likely that *snt2* is not necessary for nitrogen utilization.

DISCUSSION

In this study, we analysed the genetic and phenotypic nature of the FOM mutant (D122) isolated on the basis of its reduced pathogenicity.

The D122 mutant was found to be disrupted in the *snt2* gene encoding a protein homologous to *S. pombe* Snt2p. Snt2p is a functional part of the Lid2p complex, which is only found in fission, but not budding, yeast, and is thought to be involved in the regulation of chromatin remodelling (Roguev *et al*., 2004). The annotation of *snt2* identified several differences between the sequence in FOM and its closest relative FOL, expressed in changes in the Snt2 domain structures, probably as a result of errors in the computational annotation of the FOL gene (annotation problems may also have affected the *F. graminearum snt2* homologue gene call; such discrepancies may be resolved once appropriate cDNAs are analysed in different *Fusarium* species). The Snt2 protein of FOM carries five conserved domains: BAH, three PHDs and a GATA-type Zn finger. A multiple alignment analysis of Snt2 demonstrated a high degree of identity (63%–96%) among annotated *Fusarium* species, as well as between FOM and fungi from different genera (Fig. 2). A high degree of similarity in Snt2 architecture was observed between Snt2 proteins of FOM and the plant and human pathogens *Ustilago maydis* (XP_761724), *Candida albicans* (XP_716567) and ZNF1 (AAN75722) of the human pathogen *Cryptococcus neoformans*, involved in the pheromone response pathway (Lengeler *et al*., 2002). Most of the examined Snt2 proteins are characterized by the presence of the SANT domain, known to be an essential part of chromatin remodelling enzymes (Boyer *et al*., 2002). However, it is absent from the predicted proteins of *Fusarium, C. neoformans* and *S. pombe*. In addition, the presence of the GATA-type Zn finger, which is involved in gene expression regulation by binding promoters of various target genes, including nitrogen catabolite repression, was detected in three annotated plant pathogenic fungi, namely *F. oxysporum, Botrytis cinerea* and *Sclerotinia sclerotiorum*. Interestingly, another PHD-harbouring TF of *F. oxysporum*, FoCti6, has recently been found to be involved in fungal pathogenesis (Michielse *et al*., 2009). Similar to Snt2, Cti6 has also been found to participate in chromatin modifications.

In this study, we performed the first targeted disruption of an *snt2* TF-encoding gene in a filamentous fungus, which was not analysed in a previous high-throughput gene knockout of *N. crassa* TF-encoding genes (Colot *et al*., 2006). An unexpectedly low gene targeting efficiency (1%) was encountered in this study, even though the use of ATMT for targeted disruption has been reported to result in higher gene targeting efficiencies, ranging from 14% to 75% in different fungi, including *F. oxysporum* (Michielse *et al*., 2005). These observations could be the result of either a general difficulty in targeted integration at the *snt2* locus or a significantly slower growth rate of mutant isolates compared with ectopic transformants. Remarkably, targeted disruption of *snt2* was possible only with the GV3101 strain of *A. tumefaciens*, but not with the EHA105 strain. These data are consistent with previously reported research demonstrating that, in general, the EHA105 *Agrobacterium* strain is less suitable for targeted disruption in *F. oxysporum*, because of a relatively high percentage of false positive transformants (Khang *et al*., 2005).

snt2 was only expressed during the primary invasive growth and colonization stages of *Fusarium* wilt disease, supporting the observed delay in the appearance of the first symptoms in both *snt2* impaired mutants. At a later stage, disease progress differed between the D122 and Δ*snt2* mutants, whereby D122 caused significantly less plant mortality. The success of fungal pathogen attack frequently depends on the colonization rate of the inoculated host. In the case of FOM, the wild-type strain caused nearly 100% mortality in inoculated plants within 1 week. However, both of the *snt2* mutants did not colonize the lower and upper stem sections, in contrast with the wild-type, and rarely conferred plant mortality.

A comparative phenotypic characterization of Δ*snt2* mutants of the two Ascomycota fungi, FOM and *N. crassa*, indicated an association of the *snt2* gene with numerous developmental aspects in the tested fungi. Interestingly, in both fungi, the disruption of *snt2* caused similar sets of morphological abnormalities, including reduction in conidial production, slower vegetative growth and reduced biomass accumulation. Moreover, abnormalities were also observed in hyphal septation and in Congo red staining patterns in both FOM and *N. crassa*. Similar morphological abnormalities were observed in *Podospora anserina* during processes such as vegetative incompatibility, starvation or following treatment with a specific inhibitor of TOR kinase, rapamycin (Pinan-Lucarré *et al*., 2007). An additional trait, linking *snt2* to sexual development, was observed in Δ*snt-2 N. crassa* mutants, which produced only protoperithecia that were unable to mature. On the basis of these results, it is suggested that *snt2* functions are conserved among Ascomycota and are essential for normal fungal development. As the involvement of the *F. graminearum mgv1* gene in female fertility and pathogenesis has been demonstrated (Hou *et al*., 2002), and in the light of our data, it would be interesting to study the effect of *snt2* disruption on the pathogenicity of the head blight fungus.

In order to detect potential target genes of the Snt2 TF and to elucidate its mode of action, we combined an SSH technique with subsequent quantitative RT-PCR analysis of selected genes in both the random (D122) and targeted (Δ*snt2*) mutants, com-

pared with the wild-type isolate. Recovery of *idi4*, homologous to an autophagy regulator gene of *P. anserina*, in the suppression library was of interest, as one of the striking traits of the FOM *snt2* mutants was the increased presence of mature autophagosomes (as detected by MDC staining). As expected, the expression of *idi4* was significantly higher in both the D122 and Δ*snt2* mutants compared with the wild-type isolate. Moreover, a significant increase in expression of the *idi4* homologue of *N. crassa* (NCU08055.4) was also detected in the respective Δ*snt2* strain, suggesting a common regulatory pathway in the two fungal species.

Furthermore, it was demonstrated that the over-expression of *idi*4 led to irregularity in cell wall deposition and a reduced growth rate in *P. anserina* (Dementhon *et al*., 2004).

In this study, it was shown that, in both FOM and *N. crassa*, disruption of the *snt2* gene led to similar phenotypical abnormalities, accompanied by *idi4* over-expression. Likewise, it was demonstrated in *P. anserina* that the expression of *idi4* was up-regulated as a response to a variety of stress signals, such as oxidative, osmotic stresses, starvation and autophagy (Dementhon *et al*., 2004). Therefore, it is conceivable that the disruption of *snt2* generates a stressful intracellular environment which triggers *idi4* expression.

The autophagy process is a survival mechanism, which enables the recycling of damaged organelles or cells and supports the delicate balance between the life and death of an organism. However, autophagy has been studied extensively mainly in yeasts and mammals. In filamentous fungi, the involvement of autophagy in pathogenesis and, in particular, its regulation remain unclear (Pollack *et al*., 2009). Therefore, it is interesting that *snt2* disruptants of FOM displayed increased cell death (evident by Evans blue staining), indicating a shift in this equilibrium, implying that *snt2*, although not essential, is important for fungal survival.

In this study, four genes (i.e. *idi4, pdc, mfs* and *eEF1G*) were detected using the SSH method, and were found to be regulated by TOR kinase in the rice pathogen *F. fujikuroi* (Teichert *et al*., 2006). Furthermore, in *F. fujikuroi*, control of the AreA global nitrogen regulator via the TOR pathway may inhibit the expression of *idi4* (Schonig *et al*., 2008). TOR kinase plays an important and key role in autophagy regulation by linking nutrient sensing to cellular growth through histone acetylation (Rohde and Cardenas, 2003). An additional gene, *pdc*, involved in alcoholic fermentation, was found to be redundant in the suppression library (14%). When analysed by quantitative RT-PCR, its expression was found to be increased in the targeted Δ*snt2* mutant, compared with the wild-type isolate. In *F. fujikuroi*, *pdc* was also shown to be down-regulated by TOR kinase (Teichert *et al*., 2006). In *Aspergillus nidulans*, PDC is required for anaerobic survival of the fungus and its expression is negatively regulated by AreA (Lockington *et al*., 1997). Nevertheless, the roles of genes involved in anaerobic pyruvate assimilation and associated with pathogenicity and nitrogen metabolism are not yet clear (Bolton and Thomma, 2008). In this study, we have provided additional data supporting the probable association of pyruvate assimilation with fungal pathogenesis. These data led us to explore the possibility of Snt2 involvement in nitrogen utilization. However, no visual phenotypic difference was found when the FOM D122 and Δ*snt2* mutants were cultured on different sole nitrogen sources. Nevertheless, a significant difference in biomass accumulation, during nutrient-limiting growth conditions, may indicate a general nutrient-sensing problem. This hypothesis is supported by the evaluation of the expression of several genes involved in nitrogen metabolism (e.g. *nit4, glnA, fnr1*) in the D122 and Δ*snt2* mutants, which showed no difference from the wild-type isolate.

Hence, we conclude that Snt2 is a novel fungal TF, required for invasive growth, initial symptom development and complete pathogenicity of FOM. Snt2 is also required for the maintenance of normal morphology of at least two fungal species—FOM and *N. crassa*. Overall, the up-regulation of the autophagy-related TF-coding *idi4* gene in both FOM and *N. crassa* links *snt2* to a variety of cellular processes and is indicative of the existence of a novel, probably conserved, regulatory mechanism. Nonetheless, at this stage, more components of the Snt2 regulatory network need to be identified. In this study, we detected a unique *F. oxysporum* gene (*rbs1*), with unknown function, which appears to be up-regulated by *snt2*. Furthermore, our SSH screen results indicate that the expression of additional genes, yet to be analysed, is altered in association with this network. Finally, it is tempting to speculate that the mode of action of Snt2 in *F. oxysporum* may also involve gene expression regulation at an epigenetic level, similar to its homologue in the Lid2p complex of *S. pombe* (Li *et al*., 2008).

Nonselective autophagy and nitrogen metabolism have been shown to be connected and tightly regulated by TOR kinase (Klionsky and Emr, 2000; Teichert *et al*., 2006). *snt2* function appears to be linked to autophagosome abundance, but not to nitrogen metabolism. The fact that SNT2 and TOR kinase share common pathway components (*idi4* and *pdc*) supports the presence of an overlapping regulatory mechanism in maintaining cell survival modules.

EXPERIMENTAL PROCEDURES

Fungal strains and culture conditions

A wild-type strain of FOM (race 1,2) (Cohen *et al*., 1989) was used throughout this study. *Neurospora crassa* mutant strains were obtained from the Fungal Genetics Stock Center (Kansas, MO, USA) (McCluskey, 2003). Routinely, FOM isolates were grown in Petri dishes containing potato dextrose agar (PDA)

(Difco, Detroit, MI, USA) amended with chloramphenicol (Sigma, St. Louis, MO, USA) (0.25 mg/L). Transformants were maintained on PDA medium containing 50 mg/mL hygromycin B (Cayla, Toulouse, France). *N. crassa* isolates were maintained on Vogel's minimal medium (Davis and de Serres, 1970) and crosses were performed on cornmeal agar (CMA). All fungal isolates were purified as single spore cultures and stored at −80 °C in a 30% (v/v) glycerol solution. For *Fusarium* conidia production or DNA extraction, plugs of mycelia were cultured on *Fusarium* liquid culture (FLC) medium (Freeman *et al*., 2001) in 250-mL flasks with or without shaking (at 110 rpm), respectively. For growth rate analyses, radial growth was measured on *Fusarium* minimal medium (FMM) (Correll *et al*., 1987) with required amendments. For nitrogen utilization assessment, synthetic medium (SM) (Di Pietro and Roncero, 1996) was amended with different sole nitrogen sources at a concentration of 10 mM. The TOR kinase inhibitor, rapamycin (LC Laboratories, Woburn, MA, USA), was used at a concentration of 500 ng/mL.

Plant material and inoculation

A cultivar of muskmelon (cv. Ein Dor), susceptible to race 1,2 of FOM, which was used throughout this study, was a gift from Zeraim Gedera (Gedera, Israel). Plant inoculation assays were conducted in a glasshouse under controlled conditions at 25 ± 1°C and a 16-h light photoperiod (Freeman *et al*., 2001). Two-week-old muskmelon plants were inoculated by dipping roots for 30 min in conidial suspensions (1.5×10^6 or 5×10^5 conidia/mL), followed by transfer to water or soil medium.

Statistical analysis

All experiments were conducted at least three times. Data (apart from the results of real-time PCR) were analysed using JMP software (version 3.2.6; SAS Institute, Inc., Cary, NC, USA). All values were subjected to analysis of variance (ANOVA), and then mean comparisons of calculated values were performed and analysed using least-significant difference (LSD) analysis according to the Tukey–Kramer multiple comparison test ($P \leq 0.05$).

Nucleic acid manipulations

Genomic DNA was extracted from mycelia as described previously (Moller *et al*., 1992). For Southern hybridization, DNA was treated with appropriate restriction enzymes and analysed following standard protocols (Sambrook *et al*., 1989) using a digoxigenin-based labelling kit (Roche, Mannheim, Germany). The complete sequence of the *snt2* gene was obtained using the Genome Walking Kit (Clontech Laboratories, Mountain View, CA, USA) and wild-type DNA as a template, followed by manual annotation. Prior to total RNA extraction, harvested samples were treated with RNAlater® solution (Ambion Inc., Austin, TX, USA) and stored at −80 °C. Total RNA was extracted using the SV RNA Isolation System Kit (Promega, Madison, WI, USA). mRNA was purified using DynaBeads® (Invitrogen, Carlsbad, CA, USA). Details on the primers used throughout this research are provided in Table S1 (see Supporting Information).

Tagged and targeted mutagenesis of FOM and construction of the *snt2* disruption vector

Tagged mutagenesis of FOM was performed by ATMT using plasmids pBHt2 and pKHt kindly provided by S. Kang (Department of Plant Pathology, Pennsylvania State University, University Park, PA, USA). GV3101 and EHA105 strains of *A. tumefaciens* were used throughout this research. Transformation of FOM was carried out as described previously (Mullins *et al*., 2001) with the following modifications: 200 μL of a mixture of bacterial cells [optical density at 600 nm (OD_{600}) = 0.3] and conidia (10^5 conidia/mL) were plated directly on 12 mL of co-cultivation medium, followed by incubation at 25 °C for 48 h. Twelve millilitres of selection medium amended with 100 μg/mL hygromycin B and cefotaxime (Sanofi Aventis Laboratory, Paris, France) were overlaid on each plate and incubated at room temperature for 5–7 days. Transformants with resistance to hygromycin were maintained on PDA plates amended with hygromycin B (75 μg/mL). A collection of 2000 mitotically stable transformants was screened for pathogenicity on muskmelon plants in order to detect reduced-pathogenicity isolates. Detection of inserts in ATMT-generated transformants was performed using TAIL-PCR, following standard protocols (Mullins *et al*., 2001).

The vector for *snt2*-targeted disruption (pDΔ*snt2*) was constructed as follows. The fungal transformation vector ks:*hph* (Horowitz *et al*., 2006), containing the *Escherichia coli* hygromycin phosphotransferase (*hph*) gene regulated by the promoter from the *trp*C gene of *Aspergillus nidulans*, was used as the source of the HygB resistance cassette. A 1.7-kb fragment of *snt2* was amplified with primers homFGF1-*Sda*I/homFGR1-*Mun*I, introducing *Sda*I and *Mun*I cloning sites. This segment was cloned into pGEM-T Easy (Promega) and its 335-bp inner fragment was replaced with a 2.13-kb *hph*B/*trp*C cassette from the vector ks:*hph*, using *Acc65*I/*Bgl*II restriction. The resulting 3.8-kb *snt2*::hphR *Sda*I/*Mun*I-digested construct was transferred into *EcoR*I/*Pst*I-digested pDHt (Mullins *et al*., 2001). The targeted gene disruption event was confirmed by Southern blot analysis on *Acc65*I/*Bsp1407*I-digested genomic DNA using an inHPH-rev2/homFG1R (Table S1) PCR-amplified 1.4-kb fragment as a probe.

SSH

SSH (Diatchenko *et al*., 1996) was carried out using the Clontech PCR Select-Subtraction cDNA Kit (Clontech). For subtracted

cDNA library construction, 500-mL flasks containing 25 mL of FMM were inoculated with the wild-type and D122 strains at concentrations of 10^6 conidia/mL and incubated for 14 h on an orbital shaker at 25 °C and 100 rpm. Germinated conidia were harvested by centrifugation at 12 000 *g* for 15 min. The 'tester' sample cDNA isolated from germinated wild-type conidia, and the 'driver' sample cDNA isolated from germinated D122 strain conidia, were cloned into pGEM-T Easy (Promega) and sequenced (Macrogen Inc., Seoul, South Korea). The sequences obtained were used to search the *Fusarium* group genome database (http://www.broad.mit.edu/annotation/fgi/) and the National Center for Biotechnology Information (NCBI) database.

Gene expression analysis by quantitative RT-PCR and RT-PCR

Total RNA was extracted from cultured mycelia, germinated conidia of FOM and/or infected muskmelon seedlings. Reverse transcription was carried out on 1 μg of total RNA treated by Turbo DNase (Ambion Inc.) using Verso™ RTase (ABgene, Epsom, UK) with an anchored oligo-dT primer. cDNA was stored at −20 °C. For RT-PCR experiments, amplification was performed in 25-μL reactions with the following components: 5 μL cDNA (from the reaction mentioned above), 2.5 U Taq DNA polymerase, X1 Taq polymerase buffer, 0.2 mM deoxynucleoside triphosphates (dNTPs) and sense and anti-sense primers at final concentrations of 0.5 μM. All RNA samples were treated by DNase prior to further manipulations. Transcript levels of the selected fungal genes were analysed by quantitative RT-PCR using cDNA dilutions as templates for calibration curves. *snt2* expression *in planta* was evaluated by quantitative RT-PCR analyses using mRNA extracted from inoculated and noninoculated muskmelon seedlings at 24-h intervals from 1 to 5 dpi. cDNA obtained at 2 dpi was used as a reference (at 1 dpi no expression of the reference fungal 'housekeeping' gene was detected). Quantitative RT-PCRs were carried out in 15-μL volumes using 4 μL of cDNA, sense and anti-sense primers at final concentrations of 0.3 μM and X1 DyNamo Flash Master SYBR Green Mix (FinnEnzymes, Espoo, Finland). Quantitative RT-PCR amplification was performed using a Rotor-Gene 3000 machine (Corbett Research, Sydney, Australia). Relative quantification of a target transcript was analysed using the REST-2005© program, which is based on the mean crossing point (CP) deviation of the control and sample group, normalized by a reference (β-tubulin) transcript (Pfaffl *et al*., 2002). A Pair Wise Fixed Reallocation Randomization Test© was used to analyse the mean of at least two biological and four technical repeats with standard error, detecting the relative quantification as well as the level of significance.

Microscopy

For microscopic analyses, mycelium was grown on FMM medium for 48 h. The mycelium was examined using an inverted laser scanning confocal microscope (Olympus IX 81, Tokyo, Japan). Specific staining of mature autophagosomes was performed with 0.05 mM monodansylcadaverine (MDC) (Biederbick *et al*., 1995) with or without the addition of 1 μM of the serine protease inhibitor PMSF (Pollack *et al*., 2009). The specific autophagosome inhibitor 3-MA (Pollack *et al*., 2009) was applied at a concentration of 1 mM. For vitality staining, 0.1% Evans blue dye was applied (Dementhon *et al*., 2003). Cell wall abnormalities were detected by Congo red staining. The mycelium was overlaid with 0.1% (w/v) Congo red solution in 150 mM NaCl for 2 min and rinsed with 150 mM NaCl.

ACKNOWLEDGEMENTS

We thank Eduard Belausov for assistance with microscopy, Seogchan Kang for providing the pDHt, pBHt2 and pKHt plasmids, and Zeraim Gedera (Israel) for cv. Ein Dor muskmelon seeds. YD is a recipient of a fellowship from the Israeli Phytopathological Society.

REFERENCES

Biederbick, A., Kern, H.F. and Elsässer, H.P. (1995) Monodansylcadaverine (MDC) is a specific *in vivo* marker for autophagic vacuoles. *Eur. J. Cell Biol*. **66**, 3–14.

Bolton, M.D. and Thomma, B.P.H.J. (2008) The complexity of nitrogen metabolism and nitrogen-regulated gene expression in plant pathogenic fungi. *Physiol. Mol. Plant Pathol*. **72**, 101–110.

Boyer, L.A., Langer, M.R., Crowley, K.A., Tan, S., Denu, J.M. and Peterson, C.L. (2002) Essential role for the SANT domain in the functioning of multiple chromatin remodeling enzymes. *Mol. Cell*, **10**, 935–942.

Calero-Nieto, F., Di Pietro, A., Roncero, M.I.G. and Hera, C. (2007) Role of the transcriptional activator XlnR of *Fusarium oxysporum* in regulation of xylanase genes and virulence. *Mol. Plant–Microbe Interact*. **20**, 977–985.

Campanella, J.J., Bitincka, L. and Smalley, J. (2003) MatGAT: an application that generates similarity/identity matrices using protein or DNA sequences. *BMC Bioinformatics*, **4**, 29.

Caracuel, Z., Roncero, M.I.G., Espeso, E.A., Gonzalez-Verdejo, C.I., Garcia-Maceira, F.I. and Di Pietro, A. (2003) The pH response transcription factor PacC controls virulence in the plant pathogen *Fusarium oxysporum*. *Mol. Microbiol*. **48**, 765–779.

Cohen, R., Katan, T., Katan, J. and Cohn, R. (1989) Occurrence of *Fusarium oxysporum* f. sp. *melonis* race 1,2 on muskmelon in Israel. *Phytoparasitica*, **17**, 319–322.

Colot, H.V., Park, G., Turner, G.E., Ringelberg, C., Crew, C.M., Litvinkova, L., Weiss, R.L., Borkovich, K.A. and Dunlap, J.C. (2006) A high-throughput gene knockout procedure for *Neurospora* reveals functions for multiple transcription factors. *Proc. Natl. Acad. Sci. USA*, **103**, 10 352–11 057.

Correll, J.C., Klittich, C.J.R. and Leslie, J.F. (1987) Nitrate non-utilizing mutants of *Fusarium oxysporum* and their use in vegetative compatibility tests. *Phytopathology*, **77**, 1640–1646.

Davis, R.H. and de Serres, F.J. (1970) Genetic and microbiological research techniques for *Neurospora crassa*. *Methods Enzymol*. **27**, 79–143.

Dementhon, K., Paoletti, M., Pinan-Lucarre, B., Loubradou-Bourges, N., Sabourin, M., Saupe, S.J. and Clave, C. (2003) Rapamycin mimics the

incompatibility reaction in the fungus *Podospora anserina*. *Eukaryot. Cell*, **2**, 238–246.

Dementhon, K., Saupe, S.S. and Clave, C. (2004) Characterization of IDI-4, a b-ZIP transcription factor inducing autophagy and cell death in the fungus *Podospora anserina*. *Mol. Microbiol*. **53**, 1625–1640.

Denisov, Y., Yarden, O. and Freeman, S. (2005) Impaired purine biosynthesis affects pathogenicity of *Fusarium oxysporum* f. sp. *melonis*. *Eur. J. Plant Pathol*. **112**, 293–297.

Di Pietro, A. and Roncero, M.I.G. (1996) Endopolygalacturonase from *Fusarium oxysporum* f.sp. *lycopersici*: purification, characterization, and production during infection of tomato plants. *Phytopathology*, **86**, 1324–1330.

Di Pietro, A., Garcia-Maceira, F.I., Meglecz, E. and Roncero, M.I.G. (2001) A MAP kinase of the vascular wilt fungus *Fusarium oxysporum* is essential for root penetration and pathogenesis. *Mol. Microbiol*. **39**, 1140–1152.

Diatchenko, L., Lau, Y.-F.C., Campbell, A.P., Chenchik, A., Moqadam, F., Huang, B., Lukyanov, S., Lukyanov, K., Gurskaya, N., Sverdlov, E.D. and Siebert, P.D. (1996) Suppression subtractive hybridization: a method for generating differentially regulated or tissue-specific cDNA probes and libraries. *Proc. Natl. Acad. Sci. USA*, **93**, 6025–6030.

Divon, H.H., Ziv, C., Davydov, O., Yarden, O. and Fluhr, R. (2006) The global nitrogen regulator, FNR1, regulates nitrogen-genes and fitness during *Fusarium oxysporum* pathogenesis. *Mol. Plant–Microbe Interact*. **7**, 485–497.

Dufresne, M., Bailey, J.A., Dron, M. and Langin, T. (1998) *Clk*1, a serine/threonine protein kinase-encoding gene, is involved in pathogenicity of *Colletotrichum lindemuthianum* on common bean. *Mol. Plant–Microbe Interact*. **11**, 99–108.

Duyvesteijn, R.G.E., Wijk, R., van Boer, Y., Rep, M., Cornelissen, B.J.C. and Haring, M.A. (2005) Frp1 is a *Fusarium oxysporum* F-box protein required for pathogenicity on tomato. *Mol. Microbiol*. **57**, 1051–1063.

Freeman, S., Zveibil, A., Vintal, H. and Maymon, M. (2001) Isolation of nonpathogenic mutants of *Fusarium oxysporum* f. sp. *melonis* for biocontrol of Fusarium wilt in cucurbits. *Phytopathology*, **92**, 164–168.

Horowitz, S., Freeman, S., Zveibil, A. and Yarden, O. (2006) A defect in *nir1*, a *nirA*-like transcription factor, confers morphological abnormalities and loss of pathogenicity in *Colletotrichum acutatum*. *Mol. Plant Pathol*. **7**, 341–354.

Hou, Z., Xue, C., Peng, Y., Katan, T., Kistler, H.C. and Xu, J.R. (2002) A mitogen-activated protein kinase gene (MGV1) in *Fusarium graminearum* is required for female fertility, heterokaryon formation, and plant infection. *Mol. Plant–Microbe Interact*. **15**, 1119–1127.

Imazaki, I., Kurahashi, M., Iida, Y. and Tsuge, T. (2007) Fow2, a Zn(II)2Cys6-type transcription regulator, controls plant infection of the vascular wilt fungus *Fusarium oxysporum*. *Mol. Microbiol*. **63**, 737–753.

Inoue, I., Namiki, F. and Tsuge, T. (2002) Plant colonization by the vascular wilt fungus *Fusarium oxysporum* requires FOW1, a gene encoding a mitochondrial protein. *Plant Cell*, **14**, 1869–1883.

Khang, C.H., Park, S.Y., Lee, Y.H. and Kang, S.C. (2005) A dual selection based, targeted gene replacement tool for *Magnaporthe grisea* and *Fusarium oxysporum*. *Fungal Genet. Biol*. **42**, 483–492.

Kikuma, T., Ohneda, M., Arioka, M. and Kitamoto, K. (2006) Functional analysis of the ATG8 homologue *Aoatg8* and role of autophagy in differentiation and germination in *Aspergillus oryzae*. *Eukaryot. Cell* **8**, 1328–1336.

Kim, H. and Woloshuk, C.P. (2008) Role of AREA, a regulator of nitrogen metabolism, during colonization of maize kernels and fumonisin biosynthesis in *Fusarium verticillioides*. *Fungal Genet. Biol*. **45**, 947–953.

Klionsky, D.H. and Emr, S.D. (2000) Autophagy as a regulated pathway of cellular degradation. *Science*, **290**, 1717–1721.

Lengeler, K.B., Fox, D.S., Fraser, J.A., Allen, A., Forrester, K., Dietrich, F.S. and Heitman, J. (2002) Mating-type locus of *Cryptococcus neoformans*: a step in the evolution of sex chromosomes. *Eukaryot. Cell*, **1**, 704–718.

Levine, B. and Klionsky, D.J. (2004) Development by self-digestion: molecular mechanisms and biological functions of autophagy. *Dev. Cell*, **6**, 463–477.

Li, F., Huarte, M., Zaratiegui, M., Vaughn, M.W., Shi, Y., Martienssen, R. and Cande, W.Z. (2008) Lid2 is required for coordinating H3K4 and H3K9 methylation of heterochromatin and euchromatin. *Cell*, **135**, 272–283.

Liu, X.H., Lu, J.P. and Lin, F.C. (2007) Autophagy during conidiation, conidial germination and turgor generation in *Magnaporthe grisea*. *Autophagy*, **3**, 472–473.

Lockington, R.A., Borlace, G.N. and Kelly, J.M. (1997) Pyruvate decarboxylase and anaerobic survival in *Aspergillus nidulans*. *Gene*, **191**, 61–67.

Ma, L.J., van der Does, H.C., Borkovich, K.A., Coleman, J.J., Daboussi, M.J., Di Pietro, A., Dufresne, M., Freitag, M., Grabherr, M., Henrissat, B., Houterman, P.M., Kang, S., Shim, W.B., Woloshuk, C., Xie, X., Xu, J.R., Antoniw, J., Baker, S.E., Bluhm, B.H., Breakspear, A., Brown, D.W., Butchko, R.A., Chapman, S., Coulson, R., Coutinho, P.M., Danchin, E.G., Diener, A., Gale, L.R., Gardiner, D.M., Goff, S., Hammond-Kosack, K.E., Hilburn, K., Hua-Van, A., Jonkers, W., Kazan, K., Kodira, C.D., Koehrsen, M., Kumar, L., Lee, Y.H., Li, L., Manners, J.M., Miranda-Saavedra, D., Mukherjee, M., Park, G., Park, J., Park, S.Y., Proctor, R.H., Regev, A., Ruiz-Roldan, M.C., Sain, D., Sakthikumar, S., Sykes, S., Schwartz, D.C., Turgeon, B.G., Wapinski, I., Yoder, O., Young, S., Zeng, Q., Zhou, S., Galagan, J., Cuomo, C.A., Kistler, H.C. and Rep, M. (2010) Comparative genomics reveals mobile pathogenicity chromosomes in Fusarium. *Nature*, **464**, 367–373.

McCluskey, K. (2003) The Fungal Genetics Stock Center: from molds to molecules. *Adv. Appl. Microbiol*. **52**, 246–262.

Michielse, C.B. and Rep, M. (2009) Pathogen profile update: *Fusarium oxysporum*. *Mol. Plant Pathol*. **10**, 311–324.

Michielse, C.B., Hooykaas, P.J.J., Hondel, C.A.M.J.J. and Ram, A.F. (2005) *Agrobacterium*-mediated transformation as a tool for functional genomics in fungi. *Curr. Genet*. **48**, 1–17.

Michielse, C.B., van Wijk, R., Reijnen, L., Cornelissen, B.J.C. and Rep, M. (2009) Insight into the molecular requirements for pathogenicity of *Fusarium oxysporum* f. sp. *lycopersici* through large-scale insertional mutagenesis. *Genom. Biol*. **10**, R4.

Moller, E.M., Bahnweg, G., Sanderman, H. and Geiger, H.H. (1992) A simple and efficient protocol for isolation of high molecular weight DNA from filamentous fungi, fruit bodies and infected plant tissues. *Nucleic Acids Res*. **20**, 6115–6116.

Mullins, E.D., Chen, X., Romanie, P., Raina, R., Geiser, D.M. and Kang, S. (2001) *Agrobacterium*-mediated transformation of *Fusarium oxysporum*: an efficient tool for insertional mutagenesis and gene transfer. *Phytopathology*, **91**, 173–180.

Namiki, F., Matsunaga, M., Okuda, M., Inoue, I., Fujita, Y. and Tsuge, T. (2001) Mutation of an arginine biosynthesis gene causes reduced pathogenicity in *Fusarium oxysporum* f. sp. *melonis*. *Mol. Plant–Microbe Interact*. **14**, 580–584.

Nelson, P.E., Toussoun, T.A. and Cook, R.J. eds. (1981) *Fusarium: Disease, Biology and Taxonomy*. University Park, Pennsylvania: The Pennsylvania State University Press. 457 pp.

Pfaffl, M.W., Horgan, G.W. and Demfie, L. (2002) Relative expression software tool (REST©) for group-wise comparison and statistical analysis of relative expression results in real-time PCR. *Nucleic Acids Res*. **30**, 36–44.

Pinan-Lucarre, B., Paoletti, M., Dementhon, K., Coulary-Salin, B. and Clave, C. (2003) Autophagy is induced during cell death by incompatibility and is essential for differentiation in the filamentous fungus *Podospora anserina*. *Mol. Microbiol*. **47**, 321–333.

Pinan-Lucarré, B., Paoletti, M. and Clave, C. (2007) Cell death by incompatibility in the fungus *Podospora*. *Semin. Cancer Biol*. **17**, 101–111.

Pollack, J.K., Harris, S.D. and Marten, M.R. (2009) Autophagy in filamentous fungi. *Fungal Genet. Biol*. **46**, 1–8.

Ramos, B., Alves-Santos, F.M., García-Sanchez, M.A., Martín-Rodrigues, N., Eslava, A.P. and Díaz-Mínguez, J.M. (2007) The gene coding for a new transcription factor (ftf1) of *Fusarium oxysporum* is only expressed during infection of common bean. *Fungal Genet. Biol*. **44**, 864–876.

Rep, M., Meijer, M., Houterman, P.M., van der Does, H.C. and Cornelissen, B.J.C. (2005) *Fusarium oxysporum* evades I-3-mediated resistance without altering the matching avirulence gene. *Mol. Plant–Microbe Interact*. **18**, 15–23.

Roguev, A., Shevchenko, A., Schaft, D., Thomas, H., Stewart, A.F. and Shevchenko, A. (2004) A comparative analysis of an orthologous proteomic

environment in the yeasts *Saccharomyces cerevisiae* and *Schizosaccharomyces pombe*. *Mol*. *Cell*. *Proteom*. **3**, 125–132.

Rohde, J.R. and Cardenas, M.E. (2003) The Tor pathway regulates gene expression by linking nutrient sensing to histone acetylation. *Mol*. *Cell Biol*. **23**, 629–635.

Rohde, J.R., Heitman, J. and Cardenas, M.E. (2001) The TOR kinases link nutrient sensing to cell growth. *J*. *Biol*. *Chem*. **276**, 9583–9586.

Sambrook, J., Fritsch, E.F. and Maniatis, T. (1989) *Molecular Cloning: A Laboratory Manual*, 2nd edn. Cold Spring Harbor, NY: Cold Spring Harbor Laboratory.

Schonig, B., Brown, D.W., Oeser, B. and Tudzynski, B. (2008) Cross-species hybridization with *Fusarium verticillioides* microarrays reveals new insights into *Fusarium fujikuroi* nitrogen regulation and the role of AreA and NMR. *Eukaryot*. *Cell*, **7**, 1831–1846.

Teichert, S., Wottawa, M., Schonig, B. and Tudzynski, B. (2006) Role of the *Fusarium fujikuroi* TOR kinase in nitrogen regulation and secondary metabolism. *Eukaryot*. *Cell*, **5**, 1807–1819.

Veneault-Fourrey, C., Barooah, M., Egan, M., Wakley, G. and Talbot, N.J. (2006) Autophagic fungal cell death is necessary for infection by the rice blast fungus. *Science*, **312**, 580–583.

SUPPORTING INFORMATION

Additional Supporting Information may be found in the online version of this article:

Fig. S1 The *snt2* strain of *Neurospora crassa* is impaired in aerial hyphae production and conidiation. On solid medium, the Δ*snt2* strain (B) developed thicker, slower growing mycelium, with few aerial hyphae, reduced numbers of conidia and therefore a less pronounced orange-coloured culture, compared with the corresponding wild-type isolate (A).
Table S1 Primers used in this study.

Please note: Wiley-Blackwell are not responsible for the content or functionality of any supporting materials supplied by the authors. Any queries (other than missing material) should be directed to the corresponding author for the article.